Naval Research Laboratory

Washington, DC 20375-5320

NRL/MR/6790--96-7816

Laser Driven Electron Acceleration in Vacuum, Gases and Plasmas

PHILLIP SPRANGLE
ERIC ESAREY
JONATHAN KRALL

Beam Physics Branch
Plasma Physics Division

April 19, 1996

Approved for public release; distribution unlimited

19960610 130

DISCLAIMER NOTICE

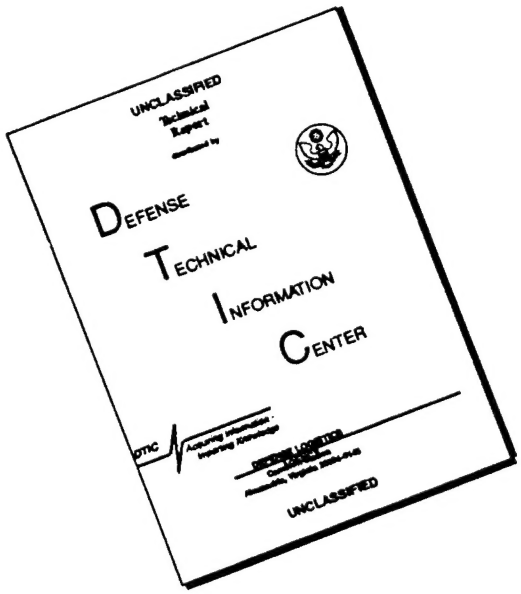

THIS DOCUMENT IS BEST QUALITY AVAILABLE. THE COPY FURNISHED TO DTIC CONTAINED A SIGNIFICANT NUMBER OF PAGES WHICH DO NOT REPRODUCE LEGIBLY.

REPORT DOCUMENTATION PAGE

Form Approved
OMB No. 0704-0188

Public reporting burden for this collection of information is estimated to average 1 hour per response, including the time for reviewing instructions, searching existing data sources, gathering and maintaining the data needed, and completing and reviewing the collection of information. Send comments regarding this burden estimate or any other aspect of this collection of information, including suggestions for reducing this burden, to Washington Headquarters Services, Directorate for Information Operations and Reports, 1215 Jefferson Davis Highway, Suite 1204, Arlington, VA 22202-4302, and to the Office of Management and Budget. Paperwork Reduction Project (0704-0188), Washington, DC 20503.

1. AGENCY USE ONLY (*Leave Blank*)	2. REPORT DATE	3. REPORT TYPE AND DATES COVERED
	April 19, 1996	Interim

4. TITLE AND SUBTITLE

Laser Driven Electron Acceleration in Vacuum, Gases and Plasmas

5. FUNDING NUMBERS

67-0899-06

6. AUTHOR(S)

Phillip Sprangle, Eric Esarey, and Jonathan Krall

7. PERFORMING ORGANIZATION NAME(S) AND ADDRESS(ES)

Naval Research Laboratory
Washington, DC 20375-5320

8. PERFORMING ORGANIZATION REPORT NUMBER

NRL/MR/6790–96-7816

9. SPONSORING/MONITORING AGENCY NAME(S) AND ADDRESS(ES)

Office of Naval Research
Arlington, VA 22217-5660

U.S. Department of Energy
Washington, DC 20585

10. SPONSORING/MONITORING AGENCY REPORT NUMBER

11. SUPPLEMENTARY NOTES

12a. DISTRIBUTION/AVAILABILITY STATEMENT

Approved for public release; distribution unlimited.

12b. DISTRIBUTION CODE

13. ABSTRACT (*Maximum 200 words*)

This paper discusses some of the important issues pertaining to laser acceleration in vacuum, neutral gases and plasmas. The limitations of laser vacuum acceleration as they relate to electron slippage, laser diffraction, material damage and electron aperture effects, are discussed. An inverse Cherenkov laser acceleration configuration is presented in which a laser beam is self-guided in a partially ionized gas. Optical self-guiding is the result of a balance between the nonlinear self-focusing properties of neutral gases and the diffraction effects of ionization. The stability of self-guided beams is analyzed and discussed. In addition, aspects of the laser wakefield accelerator are presented and laser driven accelerator experiments are briefly discussed.

14. SUBJECT TERMS

Lasers
Accelerators
Laser acceleration
Self-focusing

15. NUMBER OF PAGES

37

16. PRICE CODE

17. SECURITY CLASSIFICATION OF REPORT	18. SECURITY CLASSIFICATION OF THIS PAGE	19. SECURITY CLASSIFICATION OF ABSTRACT	20. LIMITATION OF ABSTRACT
UNCLASSIFIED	UNCLASSIFIED	UNCLASSIFIED	UL

NSN 7540-01-280-5500

Standard Form 298 (Rev. 2-89)
Prescribed by ANSI Std 239-18
298-102

CONTENTS

LASER DRIVEN ELECTRON ACCELERATION IN VACUUM, GASES AND PLASMAS

I. INTRODUCTION

Breakdown and thermal limitations in the cavities of radio frequency linacs limit the accelerating gradient to $\lesssim$ 50 MV/m. Intense focused optical beams, on the other hand, can reach field levels greater than 10^{12} V/m in vacuum. Such enormous fields have stimulated a great deal of research in laser driven acceleration concepts.[1] This paper will discuss laser acceleration of electrons in i) vacuum,[2-8] ii) neutral gases (inverse Cherenkov acceleration),[9-11] and iii) plasmas (laser wakefield acceleration).[12-25]

Advances in laser technology[26,27] have made possible compact terawatt laser systems with high intensities ($\gtrsim 10^{18}$ W/cm^2), modest energies ($\lesssim$ 100 J), and short pulses ($\lesssim$ 1 psec). The peak amplitude of the transverse electric field of a linearly polarized laser pulse is given by

$$E_L[\mathrm{TV/m}] = 2.7 \times 10^{-9} I^{1/2}[\mathrm{W/cm^2}] = 3.2\, a_o/\lambda[\mu\mathrm{m}], \qquad (1)$$

where I is the laser intensity, λ is the laser wavelength, and a_o is the laser strength parameter. Physically, a_o is the normalized transverse oscillation momentum of the electrons in the laser field. The power of a linearly polarized, Gaussian laser pulse is $P[\mathrm{GW}] = 21.5(a_o r_o/\lambda)^2$, where r_o is the minimum spot size.

II. LASER ACCELERATION IN VACUUM

The acceleration of electrons in vacuum[2-8] by optical fields is limited by diffraction effects and by electron slippage. The phase velocity of the optical field co-propagating in the direction of the accelerated electrons is greater than c and given approximately by $v_{ph}/c \simeq 1 + 1/(kZ_R)$, where $\omega = ck$ is the laser frequency, $Z_R = kr_o^2/2$ is the

Manuscript approved February 8, 1996.

Rayleigh length, i.e., Z_R is the distance over which the spot size expands. Since $v_{ph} > c$, electrons with $v_z \simeq c$ will phase slip with respect to the accelerating field and decelerate. This will occur over a slippage distance z_s, which for highly relativistic electrons is $\sim Z_R$.

A simple calculation based on Maxwell's equations in vacuum shows that under certain restrictive conditions no net energy gain is possible using optical fields. This has become known as the Lawson-Woodward (LW) theorem.[2-8] The LW theorem assumes:[2,3] (i) the region of interaction is infinite, (ii) the laser fields are in vacuum with no walls or boundaries present, (iii) the electron is highly relativistic ($v \simeq c$) along the acceleration path, (iv) no static electric or magnetic fields are present, and (v) nonlinear effects (e.g., ponderomotive, $v \times B$, and radiation reaction forces) are neglected. One or more of the assumptions of LW theorem must be violated in order to achieve a nonzero net energy gain. For example, finite energy gain can be achieved by introducing a background of gas into the interaction region, as in the inverse Cherenkov accelerator.[9-11] The gas can reduce the phase velocity of the optical beam to less than c, reducing the slippage, but diffraction remains a limitation. Alternatively, acceleration can result from the introduction of a periodic magnetic wiggler field, as in the inverse free electron laser.[28-31] In vacuum, a nonzero energy gain can be achieved by the introduction of boundaries which limit the interaction distance to a region ($\sim z_s$) about the laser focus.

A. Acceleration Using Higher Order Gaussian Beams

Higher order Gaussian modes can, in principle, provide an axial electric field component E_z for electron acceleration in vacuum.[5-8] By

properly choosing the electron injection point, net acceleration is possible. Consider a radially polarized higher order Gaussian mode propagating along the z-axis in the positive z-direction, after having been reflected off a mirror located at some negative z-position, as shown in Fig. 1. The results can be readily generalized to describe more complicated configurations. Near the axis, $E_r = E_1(rr_o/r_s^2)\sin\psi$ and $E_z = E_1(2r_o/kr_s^2)\cos\psi$, where $\psi = kz - \omega t - 2\tan^{-1}(z/Z_R)$, $r_s = r_o(1 + z^2/Z_R^2)^{1/2}$ is the laser spot size, $Z_R = \pi r_o^2/\lambda$, and E_1 is a constant. The phase velocity along the axis (r = 0) and near the focal point, $|z| \lesssim Z_R$, is given by $v_{ph}/c \simeq 1 + 1/(2\gamma_c^2)$, where $\gamma_c = \pi r_o/\sqrt{2}\lambda$ defines a critical energy. The slippage distance,[7,8] z_s, defined as the distance required for the electron to phase slip by π, is given by $\omega z_s|v_{ph}^{-1} - v_z^{-1}| \simeq \pi$,

$$z_s \simeq (\pi Z_R/2)(1 + \gamma_c^2/\gamma^2)^{-1}, \qquad (2)$$

where $\gamma = (1 - v_z^2/c^2)^{-1/2}$. In the high energy limit ($\gamma \gg \gamma_c$), $z_s \simeq \pi Z_R/2$ and in the low energy limit ($\gamma \ll \gamma_c$), $z_s \simeq \lambda\gamma^2 \ll Z_R$. Figure 2 shows the accelerating field as a function of axial distance for high (solid curve) and low (dashed curve) energy injection. In both cases, the total area under the curve is zero, i.e., there is no net energy gain from $-\infty < z < \infty$.

For a finite interaction region centered about the origin, the maximum energy gain[7,8] ΔW is given approximately by the peak amplitude of the axial electric field, $2E_o/kr_o$, multiplied by the slippage distance, z_s, i.e.,

$$\Delta W[\text{MeV}] \simeq 31P^{1/2}[\text{TW}](1 + \gamma_c^2/\gamma^2)^{-1}, \qquad (3)$$

where $P = cE_1^2r_o^2/32$ is the laser power. The critical energy $W_c \simeq mc^2\gamma_c$, can be written as $W_c[\text{MeV}] \simeq 1.1(r_o/\lambda)$. In the high energy limit ($\gamma \gg \gamma_c$), the

energy gain can be substantial, i.e., $\Delta W \simeq 100$ MeV for P = 10 TW. In the low energy limit, however, this energy gain is reduced by the factor $\gamma^2/\gamma_c^2 << 1$. When damage thresholds are considered, the low energy limit $\gamma << \gamma_c$ appears to be the relevant regime for typical parameters of interest.

B. Limitations Due to Material Damage

In principle, limiting the interaction distance to a small region near the focus can lead to substantial energy gains. In practice, however, the energy gain can be limited by the intensity damage threshold of the reflecting surface material.[8] As an example, consider placing a mirror at a distance $-z_s/2$ from the focus (z = 0) and using the higher order Gaussian mode, see Fig. 1. The electron energy gain is one-half the value given by Eq. (3).

The laser intensity on the surface of the mirror I_s must be less than the damage threshold limit, $I_s \simeq P/(\pi r_m^2) < I_d$, where r_m is the radiation spot size on the mirror surface and I_d is the mirror damage threshold intensity. Typically,[32,33] for a 1 ps laser pulse, $I_d \lesssim 5$ TW/cm^2. Since $z_s \lesssim Z_R$, $r_m \simeq r_o$. Hence, for a fixed laser power, $I_s \lesssim I_d$ implies $r_o \gtrsim (P/\pi I_d)^{1/2}$. Increasing r_o increases the critical energy, since $\gamma_c \simeq \pi r_o/(\sqrt{2}\lambda)$. The condition $I_s < I_d$ implies $\gamma_c^2 > \pi P/(2I_d\lambda^2)$, which corresponds to a critical energy $W_c \simeq mc^2\gamma_c$, $W_c[\text{GeV}] = (6.4/\lambda[\mu\text{m}])(P[\text{TW}]/I_d[\text{TW/cm}^2])^{1/2}$. Typically, this value of W_c is quite high. For P = 10 TW, λ = 1 μm, and I_d = 5 TW/cm^2, the injected beam energy should be greater than W_c = 9 GeV to be in the high energy limit. On the other hand, if the injected energy is below this critical value, the energy gain is one-half that given by Eq. (3) with $\gamma << \gamma_c$. For λ = 1 μm, P = 10 TW, I_d = 5 TW/cm^2

and W_I = 1 GeV, the energy gain is small, $\Delta W < 0.6$ MeV. These same arguments regarding the damage threshold can be applied to other laser acceleration configurations in vacuum which rely on limiting the interaction region by using optical components.

C. Limitations Due to Apertures

To limit the electron and optical beam interaction distance within an acceleration stage, the electron bunch must propagate through an aperture and the optical beam reflected, see Fig. 1. A portion of the self-fields associated with the electron bunch extends beyond the aperture and will essentially be reflected by the boundary (dielectric mirror). A limit on the maximum accelerated charge per bunch is reached when the reflected self-field energy equals the energy gain per stage or when the self-fields on the reflecting boundary become comparable to the damage threshold value. The self-fields associated with a highly relativistic electron are dominated by the radial electric field E_r and azimuthal magnetic field B_θ, i.e., the radial electric field is larger than the axial electric field by the factor γ^3. The self-fields for a single electron of charge q, at position r = 0, and $z = z_o + v_z t$, is $E_{r,1} = q\gamma r(r^2 + \gamma^2(z-z_o)^2)^{-3/2}$ and $B_{\theta,1} = (v_z/c)\, E_{r,1}$. The radial field of an electron bunch of length ℓ_b, radius r_b and consisting of N electrons, evaluated at z = 0 (midplane of bunch) and $r > r_b \ll \gamma\ell_b$ is

$$E_r = (N/\ell_b) \int_{-\ell_b/2}^{\ell_b/2} dz_o E_{r,1} = qN(\gamma/r)(r^2 + \gamma^2\ell_b^2/4)^{-1/2}. \qquad (4)$$

The total self-field energy which intercepts the boundary is given approximately by

$$W_{self} \simeq \int_{r_a}^{\infty} r dr \int_{-z_b/2}^{z_b/2} dz\, E_r^2/2$$

$$= (q^2N^2/\ell_b)\left(2\ell n\left((1 + x_a^2)^{1/2}/x_a\right) + \pi/2 - \tan^{-1}x_a\right), \quad (5)$$

where $z_b = \ell_b + r/\gamma$, r_a is the aperture radius, $r_a >> r_b$, and $x_a = 2r_a/(\gamma\ell_b)$. The fact that the radial self-field of a single electron is confined within an angle $1/\gamma$ is apparent in the limits of integration over z in Eq (5). The self-field energy intercepting the aperture in the extended electron bunch limit, $\ell_b >> 2r_a/\gamma$, is

$$W_{self} \simeq (q^2N^2/\ell_b)\left(2\ell n(\gamma\ell_b/2r_a) + \pi/2\right), \quad (6)$$

and in the localized electron bunch limit, $\ell_b << 2r_a/\gamma$, is $W_{self} \simeq q^2N^2\gamma/2r_a$.

Equating the total energy gain per stage ($N\Delta W$) with the total reflected self-field energy (RW_{self}) places a limit on the amount of charge which can be accelerated, where ΔW is the single electron energy gain per stage and R is the self-field energy reflection coefficient. The reflection coefficient is approximately given by $R = \left|(1 - \sqrt{\varepsilon})/(1 + \sqrt{\varepsilon})\right|^2$, where ε is the dielectric constant of the reflecting surface and is taken to be independent of frequency even though the self-fields have a frequency spectrum which peaks around $\simeq \pi c/\ell_b$. In the extended electron bunch limit the maximum number of electrons which can be accelerated to energy γmc^2 is

$$N_{max} = (\ell_b/r_e)(\Delta\gamma/2R)\left(\ell n(\ell_b\gamma/2r_a) + \pi/4\right)^{-1}, \quad (7)$$

and in the localized electron bunch limit is $N_{max} = (2r_a/r_e)(\Delta\gamma/\gamma)/R$ where $r_e = q^2/mc^2$ is the classical electron radius and $\Delta\gamma = \Delta W/mc^2$. For highlyrelativistic beams, the extended bunch limit is relevant, $\ell_b >> r_a/\gamma$. As an example, consider a 10 GeV electron bunch ($\gamma = 2 \times 10^4$) with $\ell_b = 0.1$ μm, $\Delta\gamma = 1$, R = 0.5, and $r_a = 5$ μm. Equation (7) yields $N_{max} \simeq 6 \times 10^6$, whereas the peak self-field at the edge of the aperture is ≃ 30 GV/m, as obtained from Eq. (4) with $N = 6 \times 10^6$. This self-field level exceeds typical damage threshold values, which are ~ 1 GV/m.

D. Vacuum Beat Wave Accelerator

The vacuum beat wave accelerator (VBWA) is an example of an accelerator based on the nonlinear ponderomotive force.[7,8] In the VBWA, two laser beams of different wavelengths, λ_1 and λ_2, are co-propagated in the presence of an injected electron beam. Properly phased electrons, traveling essentially along the same axis as the two laser beams, experience an axial acceleration from the beat term in the $\underset{\sim}{v} \times \underset{\sim}{B}$ force. By adjusting the wavelengths and spot sizes of the laser beams, the phase velocity of the ponderomotive beat wave can be adjusted such that $v_{ph} \leq c$. The acceleration mechanism in the VBWA is similar to that of the inverse free electron laser.[28-31] The energy gain in the VBWA is given by[7,8]

$$W_F[\text{MeV}] = \left[W_I^2[\text{MeV}] + 480(\lambda_1/\lambda_2 - 1)P_1[\text{TW}]\right]^{1/2}. \qquad (8)$$

where W_F (W_I) is the final (initial) electron energy and we assumed $W_I >> mc^2$. As an illustration, for $\lambda_1 = 2\lambda_2 = 1$ μm and $P_1 = 20$ TW, the energy gain is 100 MeV.

III. LASER ACCELERATION IN A GAS

The linear dispersion relation for a laser beam propagating in a neutral gas implies an axial phase velocity v_{ph} given by $v_{ph}/c \simeq 1 + 1/kZ_R - (\eta_o^2 - 1)/2$, where η_o is the linear refractive index. Typically, $\eta_o^2 - 1 \ll 1$ and is proportional to the neutral gas density n_n. Proper choice of n_n can result in $v_{ph} \leq c$ and electron phase slippage can be eliminated, however, diffraction remains an important limitation. This is the basis of the inverse Cherenkov accelerator (ICA),[9-11] which uses a higher order Gaussian laser beam to accelerate electrons in a gas. Experiments at BNL[10] on the conventional ICA observed a 3.7 MeV energy gain (31 MeV/m) of an injected electron beam (40 MeV) using a 580 MW CO_2 laser in 2.2 atm of H_2 gas.

A. Self-Guided Inverse Cherenkov Acceleration

In the conventional ICA, the electron accelerating distance (energy gain) is severely limited by diffraction effects. By self-guiding the optical beam in the ICA,[11] substantially higher electron energy gains can be achieved.

A self-guided inverse Cherenkov accelerator (ICA) has recently been proposed and analyzed.[11] The self-guided ICA uses a higher order Gaussian laser pulse which has a radially-polarized electric field compoment of the form $E_r \simeq E_o(\sqrt{2}r/r_s)\exp(-r^2/r_s^2 + i\psi)$ where r_s is the laser spot size and ψ is the laser phase (near the axis, $\psi \simeq kz - \omega t - 2\tan^{-1}(z/Z_R)$). In addition, there is a significant accelerating axial field peaked along the z-axis with magnitude $|E_z| \simeq 2\sqrt{2}E_o/kr_s$ where $k = 2\pi/\lambda$. The self-guided ICA configuration operates at laser powers near the critical power for self-focusing and at intensities for which the gas is slightly ionized. Figure 3 shows the radial profiles of the electric fields and plasma for the self-

guided ICA.

The propagation of intense optical beams in gases is affected by a combination of diffraction, refraction, and ionization. The refractive index is given by $\eta(r) = \eta_o + \eta_2 I(r) - \omega_p^2(r)/2\omega^2$, where $\omega_p = (4\pi q^2 n_e/m)^{1/2}$ is the electron plasma frequency, n_e is the electron plasma density, η_2 is the nonlinear refractive index, and I is the intensity of the optical beam. Generally, η_2 is positive and results in self-focusing of the optical beam when the beam power is greater than the nonlinear focusing (critical) power, which for a fundamental Gaussian beam[34] is $P_{NG} = \lambda^2/(2\pi\eta_o\eta_2)$. As the beam self-focuses the peak intensity becomes sufficiently large so that tunneling ionization occurs and a plasma is generated. The local decrease in the refractive index due to the plasma tends to defocus the optical beam. If diffraction, self-focusing due to η_2 and defocusing due to plasma generation are properly balanced, a self-guided optical beam can be formed.

An envelope equation describing the evolution of the optical beam spot size $r_s(z,t)$ can be derived by applying the source dependent expansion (SDE) method[35] to the paraxial wave equation. In the SDE method, the optical beam is expanded in a complete set of orthogonal Laguerre-Gaussian functions which are implicitly functions of $\zeta = z - ct$ and the propagation time, $\tau = t$, through the optical beam parameters, i.e., spot size, wavefront curvature, amplitude and phase. The self-guiding analysis assumes that the optical beam is adequately described by a single Laguerre-Gaussian mode and higher order mode coupling and generation are neglected. Ionization is considered in the high field limit and is modeled by the

tunneling ionization rate.[36] The evolution of the spot size $r_s(\zeta,\tau)$ is given by[11]

$$\partial^2 R/\partial\tau^2 = (c/Z_{Ro})^2 R^{-3}\left(1 - P/P_{NR} + (1/4)r_o^2 k_{pn}^2 \sigma_R R^2\right), \qquad (9)$$

where $R = r_s/r_o$ is the spot size normalized to its initial value, $Z_{Ro} = kr_o^2/2$ is the initial Rayleigh length, $P = (c\eta_o/16)E_o^2 r_o^2$ is the total power, $P_{NR} = 8\pi/(k^2\eta_o\eta_2)$ is the nonlinear focusing power for the radially polarized beam, $k_{pn}^2 = 4\pi q^2 n_n/mc^2$, and σ_R is the filling factor. The terms on the right-hand side of Eq. (9) denote respectively, vacuum diffraction, nonlinear focusing and plasma defocusing. The filling factor is given by

$$\sigma_R = \int_o^\infty dx(n_e/n_n)(2 - x)xe^{-x}, \qquad (10)$$

where $x = 2r^2/r_s^2$. In the limit $n_e/n_n << 1$, the plasma density is given by $\partial n_e/\partial\zeta = -(n_n/c)W_{ion}(|\underset{\sim}{E}|)$, where $W_{ion}(|\underset{\sim}{E}|)$ is the usual tunneling ionization rate,[36] which is a function of the field amplitude $|\underset{\sim}{E}|$.

The condition for a matched beam, i.e., $\partial^2 R/\partial\tau^2 = 0$, is given by $P/P_{NR} - 1 = k_{pn}^2 r_o^2 \sigma_R/4 \geq 0$. For a matched beam, it can be shown that the phase velocity is given by $v_{ph}/c \simeq 1 - 0.5(\lambda/\pi r_o)^2 P/P_{NR} - (\eta_o^2 - 1)/2$. Note that $v_{ph} < c$ and is determined by the linear and nonlinear refractive indices as well as the power.

The accelerating gradient $|E_z| = (\sqrt{2}/\pi)(\lambda/r_s)E_o$ can be estimated by considering the case of a matched beam i.e., $P \simeq P_{NL}$ and $\sigma_R \geq 0$. For this case we find that $E_o \simeq (8\pi eI/c)^{1/2}$, $\lambda/r_s \simeq (\pi/2)(e\eta_o\eta_2 I)^{1/2}$ and the accelerating gradient becomes

$$|E_z| = (e\eta_o\eta_2 I/2)^{1/2}E_o \simeq 2e(\pi\eta_o\eta_2 I_I/c)^{1/2} I_I^{1/2}, \qquad (11)$$

where we have set I equal to the ionization intensity ($I \simeq I_I$).

The phase velocity can be controlled by introducing a small amount of background plasma.[11] A transversely uniform background plasma will increase the phase velocity but have no effect on the focusing of the optical beam. The background plasma can be created by introducing a small concentration of easily ionized gas, i.e., low ionization intensity. In addition, the background density can be tapered as a function of z to increase the phase velocity and optimize electron acceleration.

B. Ionization-Modulation Instability

The equilibrium described above is subject to an ionization-modulation (IM) instability.[11] The IM instability is due to varying degrees of ionization along the beam and results in the modulation of the optical beam envelope. The IM instability can be analyzed by perturbing the equilibrium spot size of an optical beam, $R = R_o + \delta R$, where R_o is the equilibrium value and δR is the perturbation. Expansion of Eq. (9) about R_o indicates that the perturbed envelope satisfies an equation of the form

$$\partial^2 \delta R/\partial \tau^2 = \int_{\zeta}^{o} U(\zeta')\delta R(\zeta')d\zeta', \tag{12}$$

where U is a slowly varying function of ζ. For a fundamental Gaussian beam, it can be shown[11] that in the linear regime the asymptotic growth of the IM instability is of the form $\delta R \sim \exp[(1 \pm i\sqrt{3})N_e]$, where

$$N_e \simeq \left[k_{pn}^2 r_o^2 \left(n_e(\zeta)/n_n\right)\left(c\tau/Z_R\right)^2\right]^{1/3}. \tag{13}$$

The growth of the IM instability depends on the profile of the plasma electron density along the axis, $n_e(\zeta)$. As an example, for a gas at 20 atm

with $n_e/n_n \simeq 10^{-4}$ and $r_o \simeq 28$ μm, as in Fig. 4 discussed below, the beam undergoes approximately 25 e-folds ($N_e \sim 25$) after propagating a distance of 100 Rayleigh lengths ($c\tau = 100\ Z_R$).

To gain some understanding of the IM instability, consider increasing the spot size of a matched optical beam, i.e., $\delta R(\tau = 0) > 0$. In this case the beam intensity and ionization rate are reduced resulting in less plasma generation and focusing of the beam. The focusing optical beam overshoots its equilibrium value such that $\delta R < 0$ some distance behind the beam front. When $\delta R < 0$, the intensity, ionization rate, and plasma density increase, causing the beam to defocus and overshoot its equilibrium value. This focusing and defocusing of the beam results in the IM instability. The modulation amplitude and period are functions of the distance back from the head of the optical beam, $|\zeta|$, and the propagation distance $c\tau$.

C. Ionization and Collisional Losses

As the plasma electrons oscillate in the laser field, they can collide with the background plasma electrons, ions, and the neutral atoms. For a weakly ionized gas, electron scattering is dominated by electron-neutral collisions.[11] The electron-neutral collision frequency is given by $\nu_{en} = n_n \sigma_{en} \langle v_{os} \rangle$, where σ_{en} is the electron-neutral cross-section and $\langle v_{os} \rangle$ is an average oscillation velocity of the electrons. Typically, $\sigma_{en} \simeq \sigma_o$ is approximately constant for electron energies $\varepsilon < \varepsilon_o$, where $\sigma_o \sim 10^{-15}$ cm^{-3} and ε_o is on the order of tens of eV. For example, $n_n = 3 \times 10^{19}$ cm^{-3} and $\langle v_{os} \rangle = 5 \times 10^{-3} c$ imply an electron-neutral collision time of $\tau_{en} = \nu_{en}^{-1} \sim$ 200 fs.

Ionization of the gas as well as electron-neutral collisions result in the depletion of the laser intensity, I, which is found to be given by [11] $\partial I/\partial(c\tau) = -I/L_d$, where

$$L_d = ck^2/\left(\nu_{en}k_p^2 + W_{ion}k_{pn}^2\right)f, \tag{14}$$

is the intensity attenuation length. In Eq. (14), W_{ion} is the tunneling ionization rate,[36] $k_p = \omega_p/c$, $f = \sigma_p/\sigma_L \ll 1$, σ_p (σ_L) is the cross-sectional area of the generated plasma (laser) and the oscillation energy, $m\langle v_{os}\rangle^2/2$, is assumed large compared to the ionization energy. For $n_n = 3 \times 10^{19}$ cm^{-3}, $n_e = 10^{16}$ cm^{-3}, $\nu_{en} \simeq 5 \times 10^{12}$ s^{-1}, $W_{ion} \simeq 2 \times 10^9$ s^{-1}, $\lambda = 1$ μm, and $f \sim 10^{-1}$, the attenuation length is $L_d \sim 30$ m.

D. Numerical Examples

As an example, consider a self-guided ICA, in which a higher order, radially polarized optical beam of wavelength $\lambda = 1$ μm propagates in hydrogen (H_2) at 30 atm. Since $E_z \sim \eta_2^{1/2} \sim n_n^{1/2}$, the accelerating gradient can be increased by increasing the gas pressure. Hydrogen is chosen for its low atomic number, Z, i.e., low bremsstrahlung losses ($\sim Z^2$). At 30 atm, $n_n \simeq 8.1 \times 10^{20}$ cm^{-3}, $\eta_2 \simeq 3.3 \times 10^{-18}$ cm^2/W, $P_{NR} \simeq 1.9$ GW and ionization potential $U_I \simeq 15.4$ eV. The matched beam conditions can be determined from Eqs. (9) and (10) for a given axial intensity profile. For a constant peak intensity of $I = 4.7 \times 10^{13}$ W/cm^2, the matched profiles for the spot size r_s and the power P are shown in Fig. 4. For these parameters, the amount of ionized plasma is small, $n_e/n_n \leq 10^{-4}$. The on-axis accelerating field, also shown in Fig. 4, has the maximum value 450 MV/m at the front of the optical beam.

As discussed above the optical beam undergoes a IM instability. Numerical simulations of Eq. (9) show that, with a 1% initial perturbation

of the spot size, the IM instability significantly disrupts the beam envelope after ~ 10 cm of propagation. The growth rate of the IM instability is a highly nonlinear function of the laser intensity, through the electron density. Reducing the intensity in the example to 3.2×10^{13} W/cm^2 (which reduces E_z to 300 MeV/m) results in a matched beam with very little ionization (the plasma density is reduced by a factor of 130) and little variation in power and spot radius along the length of the laser pulse. Simulations show that with a 1% perturbation in the spot size, the pulse propagates > 1 meter without significant disruption.

A self-focusing mechanism has recently been reported with ultrashort fundamental Gaussian laser pulses.[37] In these experiments laser pulses with intensities of ~ 7×10^{13} W/cm^2 and spot sizes of ~ 40 μm were propagated over 20 m in air. This experiment, however, does not demonstrate the self-guiding of a fundamental Gaussian beam since a significant portion of the beam energy exists beyond the 40 μm spot size.

IV. LASER ACCELERATION IN PLASMAS

Plasmas can offer some advantages as an accelerating medium in laser driven accelerators. Plasmas can be modulated and sustain ultrahigh electric fields, and under appropriate conditions can optically guide the laser beam. The two laser-plasma accelerator configurations which have received the most attention are the plasma beat wave accelerator (PBWA)[12,38-41] and the laser wakefield accelerator (LWFA).[12-23] The PBWA utilizes two laser beams of frequencies ω_1 and ω_2, such that $\omega_1 - \omega_2 \simeq \omega_p$ is the plasma frequency, to resonantly drive a plasma wave. The following discussion is concerned primarily with the LWFA.

A. Laser Wakefield Acceleration

As an intense laser pulse propagates through an underdense plasma, i.e., $\lambda^2/\lambda_p^2 << 1$, where $\lambda_p = 2\pi c/\omega_p$, $\omega_p = (4\pi q^2 n_{eo}/m)^{1/2}$, and n_{eo} is the ambient electron density, the ponderomotive force associated with the laser pulse envelope, $F_p \sim \nabla a^2$, expels electrons from the region of the laser pulse. If the pulse length is approximately equal to the plasma wavelength, $c\tau_L \simeq \lambda_p$, the ponderomotive force excites large amplitude plasma waves (wakefields) with phase velocities approximately equal to the laser pulse group velocity.[12-24] The maximum wakefield amplitude generated by a linearly polarized laser pulse of amplitude a_o, in the 1-D limit $r_o^2 >> \lambda_p^2$, is[15-18]

$$E_{max}[\text{GeV/m}] = 3.8\text{x}10^{-8}(n_{eo}[\text{cm}^{-3}])^{1/2} a_o^2(1 + a_o^2/2)^{-1/2}. \quad (15)$$

In the absence of optical guiding, the interaction distance, L_{int}, will be limited by diffraction, i.e., $L_{int} \simeq \pi Z_R$. The maximum energy gain of the electron beam in a single stage is $\Delta W = E_{max} L_{int}$ which, in the limit $a_o^2 << 1$, may be written as[18] $\Delta W[\text{MeV}] = 580(\lambda/\lambda_p)P[\text{TW}]$. As an example, consider a $\tau_L = 1$ psec linearly polarized laser pulse with P = 10 TW, $\lambda = 1$ μm and $r_o = 30$ μm ($a_o = 0.72$). The requirement that $c\tau_L = \lambda_p$ implies $n_{eo} = 1.2 \times 10^{16}$ cm^{-3}. This gives $E_{max} = 2.0$ GeV/m, $L_{int} = 0.9$ cm, and $\Delta W = 18$ MeV. The interaction length and the electron energy gain may be greatly increased by optically guiding the laser pulse in the plasma.

B. Optical Guiding in Plasma

For a laser pulse to propagate in a plasma beyond the limits of vacuum diffraction, some form of optical guiding is necessary. For sufficiently powerful, long laser pulses, diffraction can be overcome by relativistic

effects and the laser pulse can be optically guided.[14,16,20,42-49] The index of refraction associated with the laser in the plasma is[16]

$$\eta_R = 1 - (1/2)(\omega_p/\omega)^2 = 1 - (1/2)(\lambda/\lambda_p)^2 \gamma^{-1} n_e/n_{eo}, \qquad (16)$$

where $n_e = n_{eo} + \delta n_e$, δn_e is the perturbed electron density, and γ is the relativistic factor of the plasma electrons. For a long laser pulse (long rise time), $c\tau_L >> \lambda_p$, it may be shown[16] that $\gamma^{-1} n_e/n_{eo} \simeq (1 + a_o^2/2)^{-1/2}$. A necessary requirement for optical guiding is that η_R have a maximum on axis, $\partial\eta_R/\partial r < 0$, which is the case for a laser intensity profile peaked on axis. Analysis indicates that the main body of a long laser pulse will be optically guided, provided the laser power P exceeds a critical value, $P > P_c$, where[42-45] $P_c[GW] = 17(\lambda_p/\lambda)^2$. As an example, for $n_{eo} = 10^{19} cm^{-3}$, $\lambda_p = 11$ μm, and $\lambda = 1$ μm, the critical laser power is $P_c = 2.1$ TW. For sufficiently short pulses, $\tau_L < 1/\omega_p$, the plasma has insufficient time to respond to the laser pulse and relativistic optical guiding does not occur.[16,20]

To optically guide short intense laser pulses in plasmas a preformed plasma density channel can be used.[18,20] The index of refraction, in the absence of relativistic effects, is given by Eq. (16) with $\gamma = 1$ and $n_e = n_e(r)$ is the electron density radial profile. Optical guiding can occur when the plasma density is minimum on-axis and analysis of the wave equation for a fixed parabolic plasma density channel indicates that optical guiding of a Gaussian laser pulse occurs when the channel density depth satisfies[18,20] $\Delta n_e \geq \Delta n_c$, where $\Delta n_c = (\pi r_e r_o^2)^{-1}$ is the critical channel depth, $\Delta n_e = n_e(r = r_o) - n_e(r = 0)$ and $r_e = q^2/mc^2$. For example, a spot size of $r_o = 30$ μm implies $\Delta n_c \simeq 10^{17}$ cm^{-3}. Simulations, which include the self-consistent evolution of the density channel, indicate that

density channels can guide short pulse lengths and high intensities.[18,20,23] Recently, the guiding of modest intensity (10^{14} W/cm^2) laser pulses in a plasma density channel formed by an axicon focus has been experimentally demonstrated.[50] Capillary discharges can also be used to create plasma density channels.[51] Optical beams propagating in plasmas can undergo a wide range of instabilities which can limit the interaction distance. These instabilities include backward and forward Raman scattering,[21,52-54] self-modulation,[19-23,55] and laser hosing.[56,57]

C. Self-Modulated Laser Wakefield Acceleration

In the recently proposed self-modulated LWFA,[22,23] enhanced electron acceleration is achieved via resonant self-modulation of the laser pulse.[19-23] This occurs when the laser pulse length is several plasma wavelengths, $c\tau_L > \lambda_p$, and the peak laser power satisfies $P \geq P_c$, where $P_c[GW] \simeq 17(\lambda_p/\lambda)^2$ is the critical power. At fixed laser parameters, both conditions can be met by choosing a sufficiently high plasma density, since $P_c \sim 1/n_{eo}$ and $\lambda_p \sim 1/n_{eo}^{1/2}$. Wakefields generated in the self-modulated regime are more than an order of magnitude greater than those generated by a laser pulse with $c\tau_L = \lambda_p/2$, assuming fixed laser parameters. Acceleration is enhanced for four reasons: (i) a higher density produces a larger wakefield, $E_z \sim n_{eo}^{1/2}$, (ii) the resonant mechanism excites larger wakefields than in the standard LWFA, (iii) since $P \geq P_c$, relativistic focusing further enhances the laser intensity, and (iv) a portion of the pulse will remain guided over several diffraction lengths, extending the acceleration distance.

The self-modulation mechanism can be understood by considering a long laser pulse $c\tau_L >> \lambda_p$, with power $P \geq P_c$, such that the body of the pulse

is relativistically guided. The leading edge of the pulse will create a low-amplitude wakefield within the remainder of the laser pulse. In the wakefield, each region of decreased density acts as a local plasma channel to enhance the relativistic focusing effect, while each region of increased density causes defocusing. This results in a low-amplitude modulation of the laser pulse at λ_p. The modulated laser pulse resonantly excites the wakefield and the process continues in an unstable manner.[55] This instability develops on a time-scale associated with laser diffraction. In the one-dimensional limit, laser pulse modulation can also occur via the usual forward Raman scattering (FRS) instability.[52,54]

The parameters used in the following fluid simulations are similar to the design parameters for the NRL LWFA experiment. A Gaussian laser pulse was assumed with λ = 1 μm, a_o = 0.96, r_o = 10 μm and $c\tau_L$ = 120 μm (400 fs), such that Z_R = 0.031 cm and P = 2 TW. The density is $n_{eo} = 1.1 \times 10^{19}$ cm^{-3} (λ_p = 10 μm), such that P_c = 1.67 TW ($P \simeq 1.2P_c$). At τ = 0 the laser pulse is outside the plasma and the plasma density is "ramped up" to reach full density at $c\tau$ = 0.1 cm ($3.2Z_R$). The laser pulse is initially converging such that in vacuum it would focus to a minimum spot size of r_o = 10 μm at the point where the plasma reaches full density (0.1 cm). The simulation continues until $c\tau$ = 0.2 cm (10 Z_R).

Figure 5 shows the normalized laser intensity $|\hat{a}_f|^2$ at $c\tau$ = 0.2 cm (at focus in vacuum, $|\hat{a}_f|^2 = a_o^2$). Several peaks in the laser intensity are observable with period ~ λ_p. The corresponding plot of the axial electric field is shown in Fig. 6. As the laser becomes fully modulated, the resonant excitation of the field becomes stronger, with the peak accelerating field increasing from $|E_z|$ = 270 GV/m at $c\tau$ = 0.15 cm to $|E_z|$ = 350 GV/m at $c\tau$ = 0.2 cm.

To study the trapping and acceleration of beam electrons by the wakefield, a test particle code is used to accelerate a distribution of non-interacting particles in the time-resolved electric and magnetic wakefields of the fluid simulation. A continuous electron beam is assumed with initial energy of 1.0 MeV and normalized emittance ε_n = 7 mm-mrad. The beam is initially converging such that in vacuum it would focus to a minimum RMS radius r_b = 350 μm at $c\tau$ = 0.1 cm. After $c\tau$ = 0.2 cm, a small fraction of the original particle distribution has been trapped and accelerated. Figure 7, which shows the peak particle energy versus $c\tau$, gives a peak energy of 113 MeV at $c\tau$ = 0.2 cm.

V. LASER-PLASMA ACCELERATION EXPERIMENTS

Laser-plasma acceleration experiments have been performed in a number of configurations and/or regimes. For example, the PBWA uses two long pulse ($c\tau_L \gg \lambda_p$) laser beams of frequencies ω_1 and ω_2, such that $\omega_1 - \omega_2 \simeq \omega_p$, to resonantly drive a plasma wave.[12,38-41] The LWFA, on the other hand, uses a single, intense laser pulse to drive a plasma wave.[12-23] The LWFA can operate in the short-pulse (standard) regime[12-18] in which $c\tau_L \simeq \lambda_p$, or in the long-pulse (self-modulated) regime[19-23] in which $c\tau_L > \lambda_p$. In the self-modulated LWFA regime, laser pulse modulation can occur by the FRS instability[52,54] and/or the envelope self-modulation instability.[55,57]

Laser acceleration of electrons in plasmas has been observed in several experiments world-wide. In an early experiment by Joshi et al.,[59] a single, long pulse CO_2 laser beam interacting with a thin Carbon foil was observed to produce 1.4 MeV electrons via the FRS instability. The pioneering PBWA experiments at UCLA[40] observed a 28 MeV energy gain (2.8 GeV/m) of an injected electron beam (2 MeV) using two CO_2 laser lines in a

plasma of density 9×10^{15} cm^{-3}. These experiments are particularly well-diagnosed and various laser-plasma phenomena have been observed. PBWA experiments at Ecole Polytechnique[41] observed a 1.4 MeV energy gain (0.6 GeV/m) of an injected electron beam (3.4 MeV) using two Nd laser lines in a plasma of density 2×10^{17} cm^{-3}. Experiments at Osaka[58] observed electron acceleration in both the standard and self-modulated LWFA experiments using a 8 TW, 1 ps laser pulse and a source of ~ 1 MeV electron from a laser-solid interaction. In the standard LWFA, an energy gain of ~ 1 MeV was observed in a plasma of density 3×10^{15} cm^{-3}; and in the self-modulated LWFA, an energy gain of 17 MeV was observed in a plasma of density 10^{19} cm^{-3}. At LLNL,[59] background plasma electrons were trapped and accelerated to 2 MeV (~ 2 GeV/m) using a 5 TW, 600 fs laser pulse in a plasma of density 2×10^{19} cm^{-3} in a self-modulated LWFA experiment. At Rutherford,[60] self-modulated LWFA experiments generated 45 MeV (~ 90 GV/m) self-trapped plasma electrons using a 20 TW, 1 ps laser pulse in a 10^{19} cm^{-3} plasma. Preliminary results from Michigan[61] report the acceleration of self-trapped plasma electrons in a self-modulated LWFA experiment.

VI. DISCUSSION

Several important issues associated with laser driver acceleration in vacuum, neutral gases and plasmas have been discussed. Laser vacuum acceleration is limited by electron slippage and diffraction effects. The slippage distance is given by Eq. (2). A general class of laser vacuum acceleration configurations requires reflecting surfaces with apertures for the electron beam. Two additional limitations apply to this class of configurations. Material damage considerations place limits on the laser intensity electron energy, current and aperture radius. As the electron beam passes through the aperture a portion of the self-fields is reflected.

This reflected self-field energy represents a loss in electron kinetic energy and places a limit on the electron energy and current. Another general class of laser vacuum accelerators, e.g., the vacuum beat wave accelerator, utilizes the nonlinear (ponderomotive) laser forces.

The electron slippage limitation can be removed by using a neutral gas for the accelerating medium. However, diffractive spreading remains an important restriction. To overcome both diffraction and slippage, a self-guided inverse Cherenkov acceleration has been proposed and analyzed. Self-guiding is the result of a balance between diffraction, nonlinear self-focusing and ionization defocusing. The envelope of the self-guided optical beam is inherently unstable due to an ionization-modulation instability. Accelerating gradients of ~ 0.5 GV/m can be achieved in the self-guided ICA.

Some important features of laser acceleration in plasmas have been reviewed, including the LWFA, optical guiding in plasmas, and the self-modulated LWFA. A simulation of the self-modulated LWFA, based on the design parameters of the NRL experiment, indicates that energy gains in excess of 100 MeV and gradients in excess of 300 GV/m are possible. Several laser-plasma experiments have demonstrated electron acceleration, with electron energies as high as 45 MeV and gradients as high as 90 GV/m.

Acknowledgments

This work was supported by the Department of Energy and the Office of Naval Research. The authors acknowledge useful discussions with B. Hafizi and A. Ting.

References

1. See, e.g., Advanced Accelerator Concepts, edited by P. Schoessow, AIP Conf. Proc. 335 (Amer. Inst. Phys., NY, 1995); Advanced Accelerator Concepts, edited by J. Wurtele, AIP Conf. Proc. No. 279 (AIP, New York, 1993).
2. J.D. Lawson, Rutherford Laboratory Report No. RL-75-043 (1975); IEEE Trans. Nucl. Sci. NS-26, 4217 (1979); P.M. Woodward, J. IEE 93, 1554 (1947).
3. R.B. Palmer, in Frontiers of Particle Beams, Lecture Notes in Physics 296, edited by M. Month and S. Turner (Springer-Verlag, Berlin, 1988), p. 607; Part. Accel. 11, 81 (1980).
4. J.A. Edighoffer and R.H. Pantell, J. Appl. Phys. 50, 6120 (1979).
5. E.J. Bochove, G.T. Moore, and M.O. Scully, Phys. Rev. A 46, 6640 (1992); M.O. Scully and M.S. Zubairy, Phys. Rev. A 44, 2656 (991).
6. L.C. Steinhauer and W.D. Kimura, J. Appl. Phys. 72, 3237 (1992).
7. P. Sprangle, E. Esarey, J. Krall, and A. Ting, accepted by Optical Communication (1995).
8. E. Esarey, P. Sprangle, and J. Krall, Phys. Rev. E, Nov (1995).
9. J.R. Fontana and R.H. Pantell, J. Appl. Phys. 54, 4285 (1983).
10. W.D. Kimura, G.H. Kim, R.D. Romea, L.C. Steinhauer, I.V. Pogorelsky, K.P. Kusche, R.C. Fernow, X. Wang, and Y. Liu, Phys. Rev. Lett. 74, 546 (1995).
11. P. Sprangle, E. Esarey, and J. Krall, "Self-Guided Propagation of Higher Order and Fundamental Gaussian Optical Beams in Gases Undergoing Ionization", to be published.
12. T. Tajima and J.M. Dawson, Phys. Rev. Lett. 43, 267 (1979).

13. L.M. Gorbunov and V.I. Kirsanov, Zh. Eksp. Teor. Fiz. 93, 509 (1987) [Sov. Phys. JETP 66, 209 (1987)].

14. P. Sprangle, E. Esarey, A. Ting, and G. Joyce, Appl. Phys. Lett 53, 2146 (1988); E. Esarey, A. Ting, P. Sprangle, and G. Joyce, Comm. Plasm. Phys. Controlled Fusion 12, 191 (1989).

15. S.V. Bulanov, V.I. Kirsanov, and A.S. Sakhanov, JETP Lett. 50, 198 (1989) [Pis'ma Zh. Eksp. Teor. Fiz. 50, 176 (1989)].

16. P. Sprangle, E. Esarey, and A. Ting, Phys. Rev. A 41, 4463 (1990); P. Sprangle, E. Esarey, and A. Ting, Phys. Rev. Lett. 64, 2011 (1990); A. Ting, E. Esarey and P. Sprangle, Phys. Fluids B2, 6 (1990).

17. V.I. Berezhiani and I.G. Murusidze, Phys. Lett. A 148, 338 (1990).

18. P. Sprangle and E. Esarey, Phys. Fluids B4, 2241 (1992).

19. N. E. Andreev, L. M. Gorbunov, V. I. Kirsanov, A. A. Pogosova, and R. R. Ramazashvili, Pis'ma Zh. Eksp. Teor. Fiz. 55, 551 (1992); N.E. Andreev, V.I. Kirsanov, and L.M. Gorbunov, Phys. Plasmas 2, 2573 (1995).

20. P. Sprangle, E. Esarey, J. Krall, and G. Joyce, Phys. Rev. Lett. 69, 2200 (1992).

21. T.M. Antonsen, Jr. and P. Mora, Phys. Rev. Lett. 69, 2204 (1992); Phys. Fluids B 5, 1440 (1993).

22. J. Krall, A. Ting, E. Esarey, and P. Sprangle, Phys. Rev. E, 48, 2157 (1993).

23. E. Esarey, P. Sprangle, J. Krall, A. Ting, and G. Joyce, Phys. Fluids B 5 (7), L 2690 (1993).

24. W.B. Mori and T. Katsouleas, in Advanced Accelerator Concepts, edited by P. Schoessow, AIP Conf. Proc. 335 (Amer. Inst. Phys., NY, 1995), p. 112; T.C. Chiou, T. Katsouleas, C. Decker, W.B. Mori, J.S. Wurtele, G. Shvets, and J.J. Su, Phys. Plasmas 2, 310 (1995).

25. J.S. Wurtele, Phys. Today 47, 33 (1994).

26. P. Maine, D. Strickland, P. Bado, M. Pessot, and G. Mourou, IEEE J. Quantum Electron. 24, 398 (1988); G. Mourou and D. Umstadter, Phys. Fluids B 4, 2315 (1992).

27. M.D. Perry and G. Mourou, Science 264, 917 (1994).

28. A.A. Kolomenskii and A.N. Lebedev, Sov. Phys. JETP 23, 733 (1966).

29. R.B. Palmer, J. Appl. Phys. 43, 3014 (1972).

30. P. Sprangle and C.M. Tang, IEEE Trans. Nucl. Sci. NS-28, 3346 (1981).

31. R.H. Pantell and T.I. Smith, Appl. Phys. Lett. 40, 753 (1982).

32. D. Du, X. Liu, G. Korn, J. Squier, and G. Mourou, Appl. Phys. Lett. 64, 3071 (1994).

33. B.C. Stuart, M.D. Feit, A.M. Rubenchik, B.W. Shore, and M.D. Perry, Phys. Rev. Lett. 74, 2248 (1995).

34. Y.R. Shen, The Principles of Nonlinear Optics (Wiley, New York, 1984); R.W. Boyd, Nonlinear Optics (Academic Press, San Diego, CA, 1993).

35. P. Sprangle, A. Ting, and C.M. Tang, Phys. Rev. Lett. 59, 202 (1987); Phys. Rev. A 36, 2773 (1987).

36. L.V. Keldysh, Sov. Phys. JETP 20, 1307 (1965) [Zh. Eksp. Teor. Fiz. 47, 1945 (1964)]; M.V. Ammosov, N.B. Delone, and V.P. Krainov, Sov. Phys. JETP 64, 1191 (1987) [Zh. Eksp. Teor. Fiz. 91, 2008 (1986)].

37. A. Braun, G. Korn, X. Liu, D. Du, J. Squier, and G. Mourou, Opt. Lett. 20, 73-75 (1995); X. Liu and D. Umstadter, in Shortwavelength V: Physics with Intense Laser Pulses, edited by M.D. Perry and P.B. Corkum (Optical Society of America, Washington, DC, 1993), vol. 17, pp. 45-49.

38. C. Joshi, W.B. Mori, T. Katsouleas, J.M. Dawson, J.M. Kindel, and D.W. Forslund, Nature 311, 525 (1984); W. Mori, C. Joshi, J.M. Dawson, D.W. Forslund and J.M. Kindel, Phys. Rev. Lett. 60, 1298 (1988).

39. C. Joshi, T. Tajima, J.M. Dawson, H.A. Baldis, and N.A. Ebrahim, Phys. Rev. Lett. 47, 1285 (1981); D.W. Forslund, J.M. Kindel, W.B. Mori, C. Joshi, and J.M. Dawson, Phys. Rev. Lett. 54, 558 (1985).

40. C.E. Clayton, K.A. Marsh, A. Dyson, M. Everett, A. Lal, W.P. Leemans, R. Williams, and C. Joshi, Phys. Rev. Lett. 70, 37 (1993); C.E. Clayton, M.J. Everett, A. Lal, D. Gordon, K.A. Marsh, and C. Joshi, Phys. Plasmas 1, 1753 (1994).

41. F. Amiranoff, J. Ardonceau, M. Bercher, D. Bernard, B. Cros, A. Debraine, J.M. Dieulot, J. Fusellier, F. Jacquet, J.M. Joly, M. Juillard, G. Matthieussent, P. Matricon, P. Mine, B. Montes, P. Mora, R. Morano, J. Morillo, F. Moulin, P. Poilleux, A. Specka, and C. Stenz, in Advanced Accelerator Concepts, edited by P. Schoessow, AIP Conf. Proc. 335 (Amer. Inst. Phys., NY, 1995), p. 612.

42. A.G. Litvak, Zh. Eksp. Teor. Fiz. 57, 629 (1969) [Sov. Phys. JETP 30, 344 (1969)].

43. C.E. Max, J. Arons, and A.B. Langdon, Phys. Rev. Lett. 33, 209 (1974).

44. P. Sprangle, C.M. Tang, and E. Esarey, IEEE Trans. Plasma Sci. PS-15, 145 (1987).

45. G.Z. Sun, E. Ott, Y.C. Lee, and P. Guzdar, Phys. Fluids 30, 526 (1987).

46. A.B. Borisov, A.V. Borovskiy, V.V. Korobkin, A.M. Prokhorov, C.K. Rhodes and O.B. Shiryaev, Phys. Rev. Lett. 65, 1753 (1990).

47. X. L. Chen and R. N. Sudan, Phys. Fluids B 5, 1336 (1993).

48. H.S. Brandi, C. Manus, G. Mainfray, T. Lehner, and G. Bonnaud, Phys. Fluids B 5, 3539 (1993); G. Bonnaud, H.S. Brandi, C. Manus, G. Mainfray, and T. Lehner, Phys. Plasmas 1, 968 (1994).

49. P. Monot, T. Auguste, P. Gibbon, F. Jakober, G. Mainfray, A. Dulieu, M. Louis-Jacquet, G. Malka, and J.L. Miquel, Phys. Rev. Lett. 74, 2953 (1995); P. Gibbon, P. Monot, T. Auguste, and G. Mainfray, Phys. Plasmas 2, 1305 (1995).

50. C.G. Durfee III and H.M. Milchberg, Phys. Rev. Lett. 71, 2409 (1993); C.G. Durfee III, J. Lynch, and H.M. Milchberg, Phys. Rev. E 51, 2368 (1995).

51. A. Zigler, Y. Ehrlich, C. Cohen, J. Krall, and P. Sprangle, to be published in J. Opt. Soc. Am. B.

52. J.F. Drake, P.K. Kaw, Y.C. Lee, G. Schmidt, C.S. Liu, and M.N. Rosenbluth, Phys. Fluids 17, 778 (1974); D.W. Forslund, J.M. Kindel, and E.L. Lindman, Phys. Fluids 18, 1002 (1975).

53. P. Sprangle and E. Esarey, Phys. Rev. Lett. 67, 2021 (1991); E. Esarey and P. Sprangle, Phys. Rev. A 45, 5872 (1992).

54. W.B. Mori, C.D. Decker, D.E. Kinkel, and T. Katsouleas, Phys. Rev. Lett. 72, 1482 (1994); C.D. Decker, W.B. Mori, and T. Katsouleas, Phys. Rev. E 50, 3338 (1994).

55. E. Esarey, J. Krall, and P. Sprangle, Phys. Rev. Lett. 72, 2887 (1994).

56. G. Shvets and J.S. Wurtele, Phys. Rev. Lett. 73, 3540 (1995).

57. P. Sprangle, J. Krall and E. Esarey, Phys. Rev. Lett. 73, 3544 (1994).

58. K. Nakajima, D. Fisher, T. Kawakubo, H. Nakanishi, A. Ogata, Y. Kato, Y. Kitagawa, R. Kodama, K. Mima, H. Shiraga, K. Suzuki, K. Yamakawa, T. Zhang, Y. Sakawa, T. Shoji, Y. Nishida, N. Yugami, M. Downer, and T. Tajima, Phys. Rev. Lett. 74, 4428 (1995); in Advanced Accelerator Concepts, edited by P. Schoessow, AIP Conf. Proc. 335 (Amer. Inst. Phys., NY, 1995), p. 145.

59. C.A. Coverdale, C.B. Darrow, C.D. Decker, W.B. Mori, K.C. Tzeng, K.A. Marsh, C.E. Clayton, and C. Joshi, Phys. Rev. Lett. 74, 4659 (1995).

60. A. Modena, Z. Najmudin, A.E. Dangor, C.E. Clayton, K.A. Marsh, C. Joshi, V. Malka, C.B. Darrow, C. Danson, D. Neely, and F.N. Walsh, Nature 337, 606 (1995).

61. R. Wagner, S.Y. Chen, A. Maksimchuk, E. Dodd, J.K. Kim, and D. Umstadter, Bull. Amer. Phys. Soc. 40, 1799 (1995).

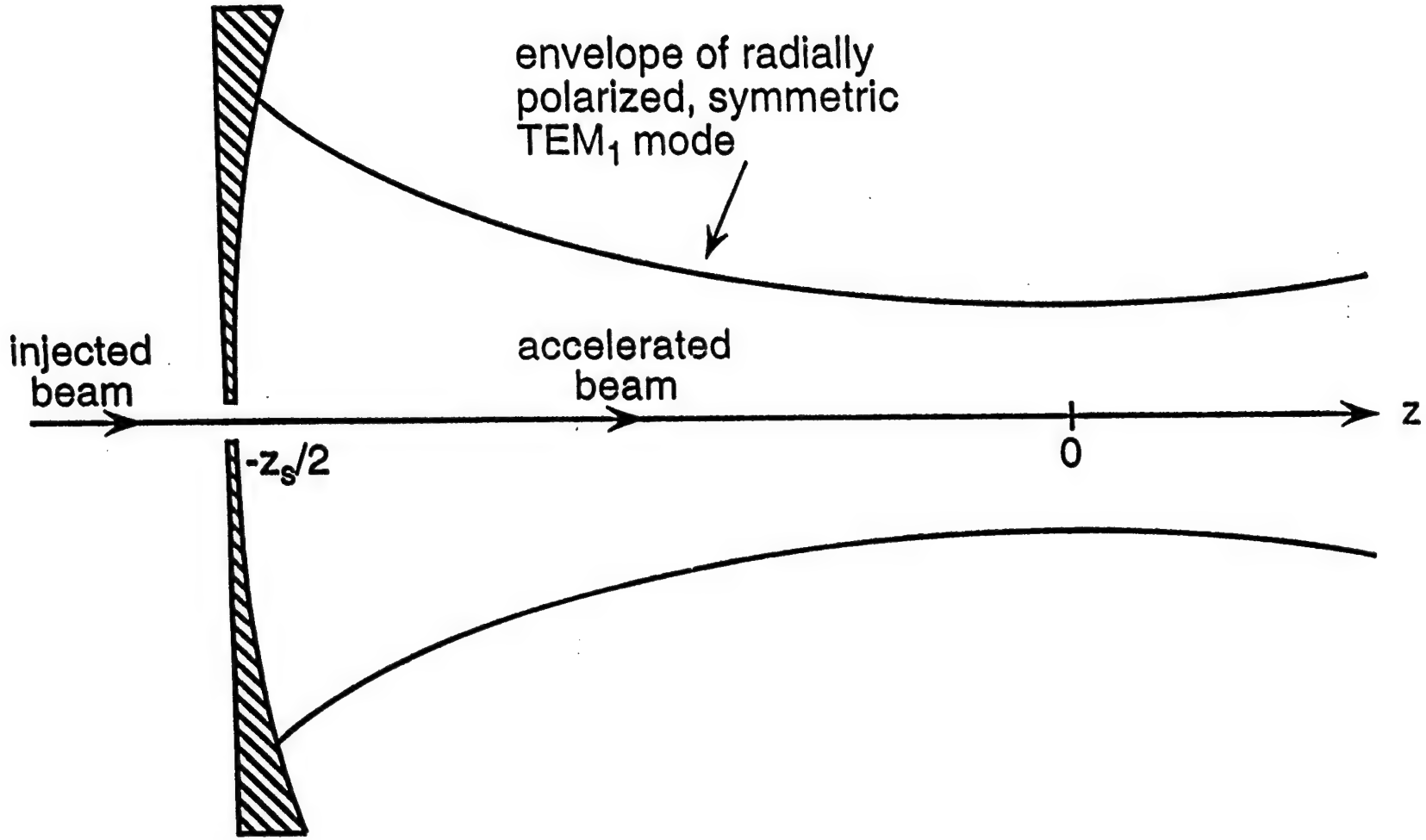

Fig. 1: Schematic of electron acceleration in vacuum by reflecting a higher order Gaussian beam from a mirror placed near focus.

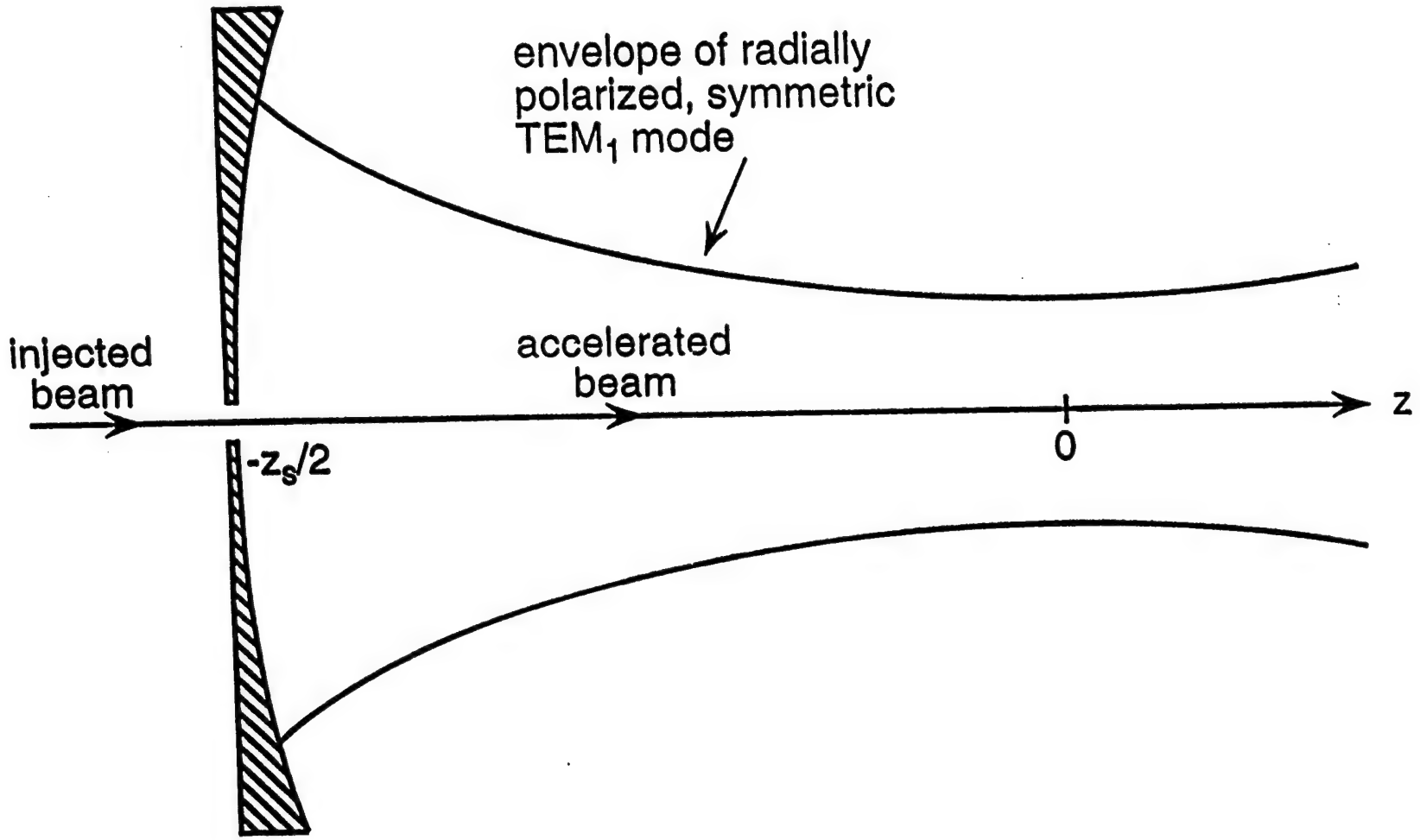

Fig. 1: Schematic of electron acceleration in vacuum by reflecting a higher order Gaussian beam from a mirror placed near focus.

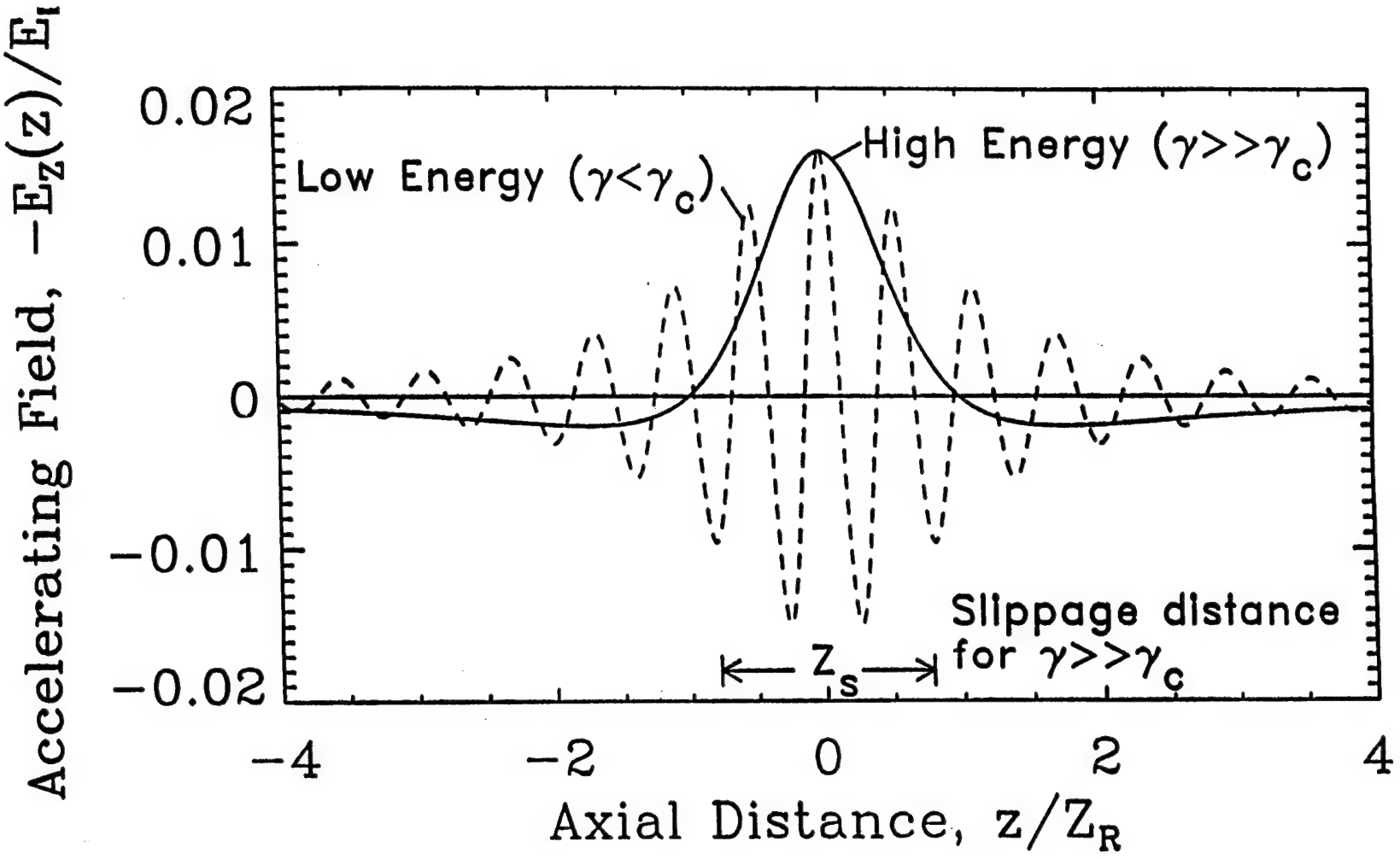

Fig. 2: Acceleration axial field $-E_z$ plotted versus position along the z-axis for the higher order Gaussian mode. The solid curve is the high energy limit $\gamma >> \gamma_c$, and the dashed curve is the low energy limit $\gamma << \gamma_c$.

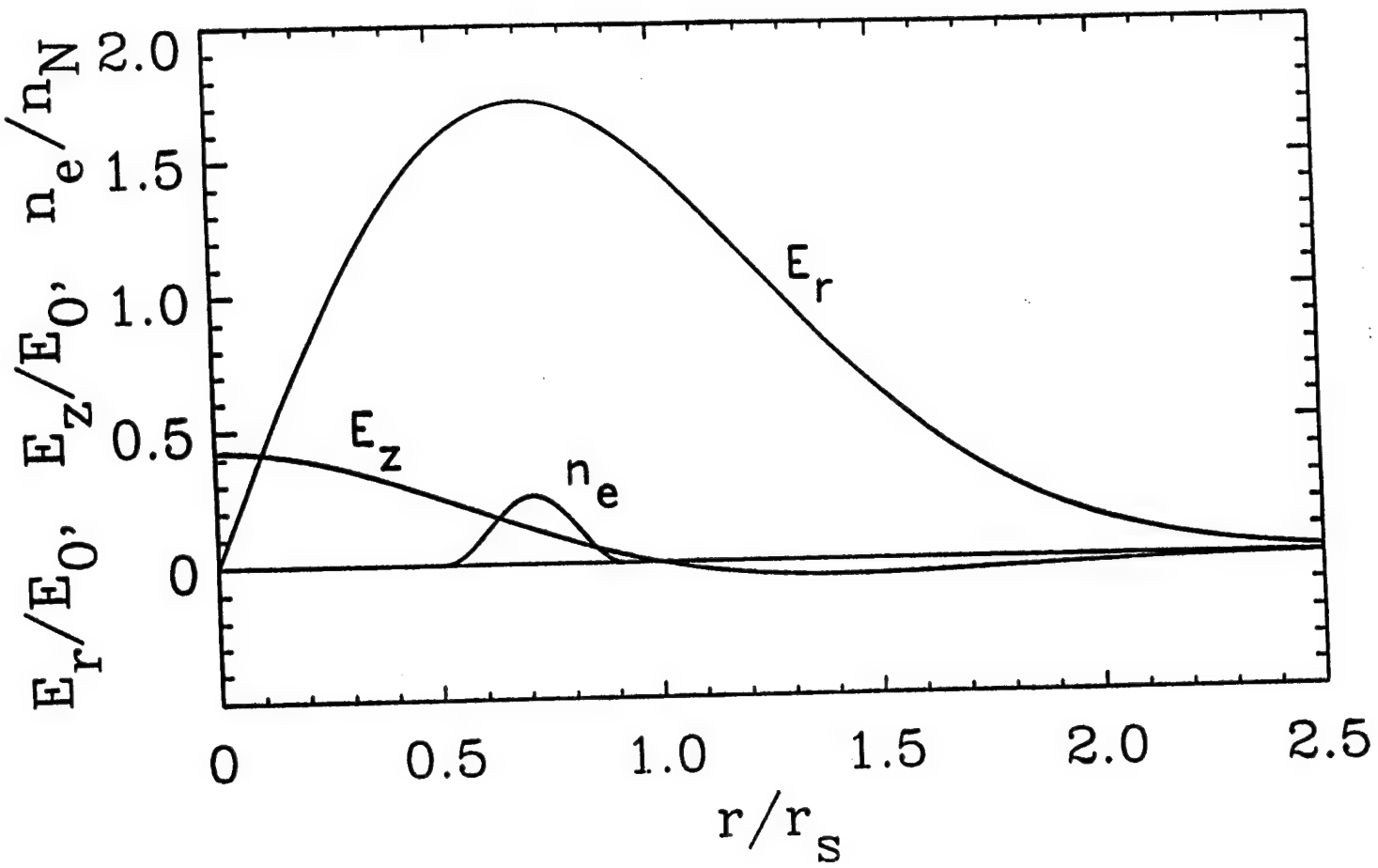

Fig. 3: Radial and axial field profiles for the radially polarized optical beam. The peak radial field $E_{r,p} = E_o/\sqrt{2}$ occurs at $r = r_s/\sqrt{2}$, the peak axial field $E_{z,p} = (\sqrt{2}/\pi)(\lambda/r_s)E_o$ occurs at $r = 0$. A plasma, with density n_e, is generated and is confined to the region $r \simeq r_s/\sqrt{2}$.

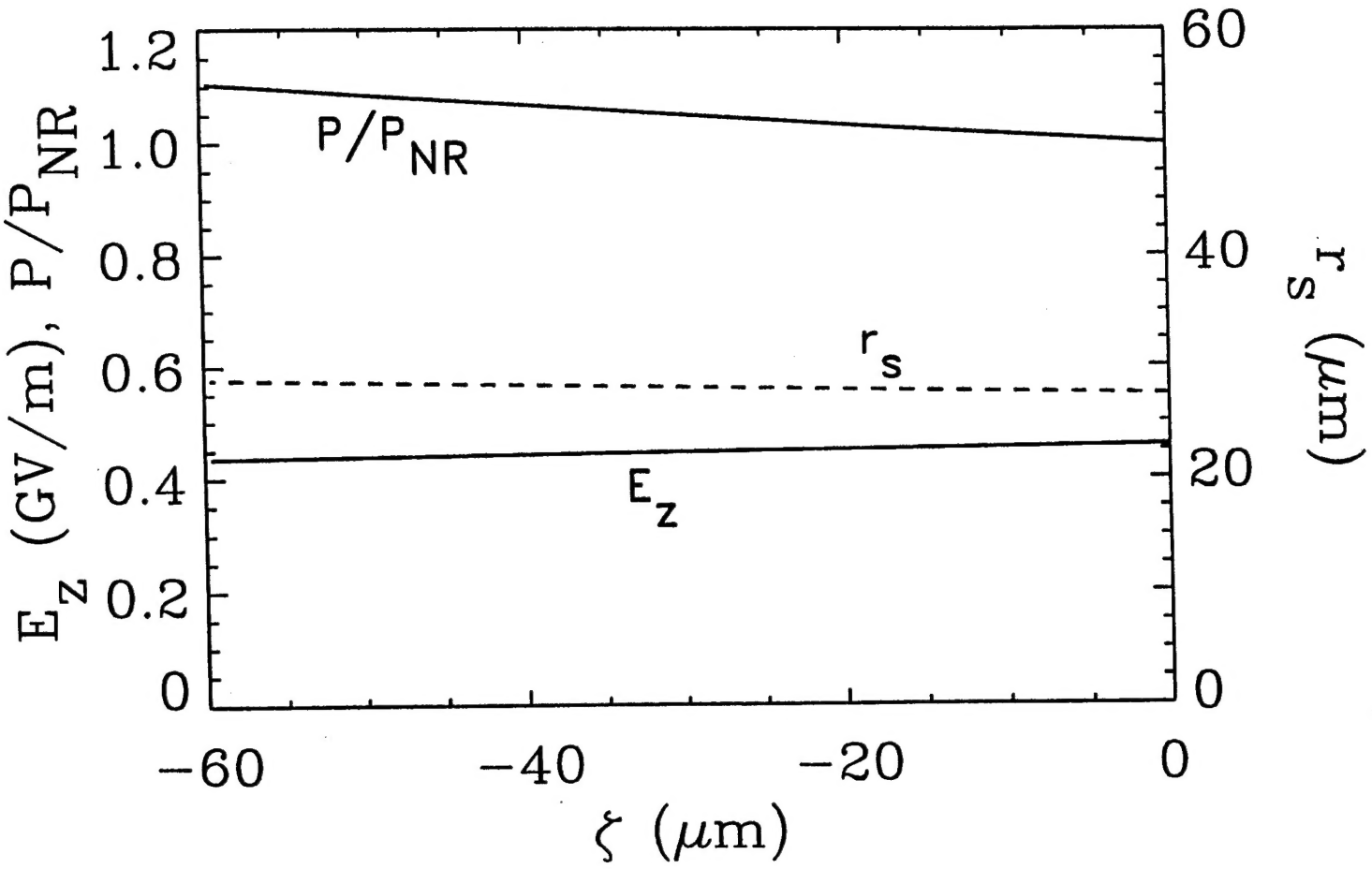

Fig. 4: Accelerating electric field E_z, spot size r_s, and power P plotted versus ζ for a matched laser pulse with wavelength $\lambda = 1$ μm propagating in hydrogen (H_2) at 30 atm: $n_n \simeq 8.1 \times 10^{20}$ cm^{-3}, $\eta_2 \simeq 3.3 \times 10^{-18}$ cm^2/W, $P_{NR} \simeq 1.9$ GW and $U_I = 15.4$ eV. The peak accelerating field is ~ 450 MV/m.

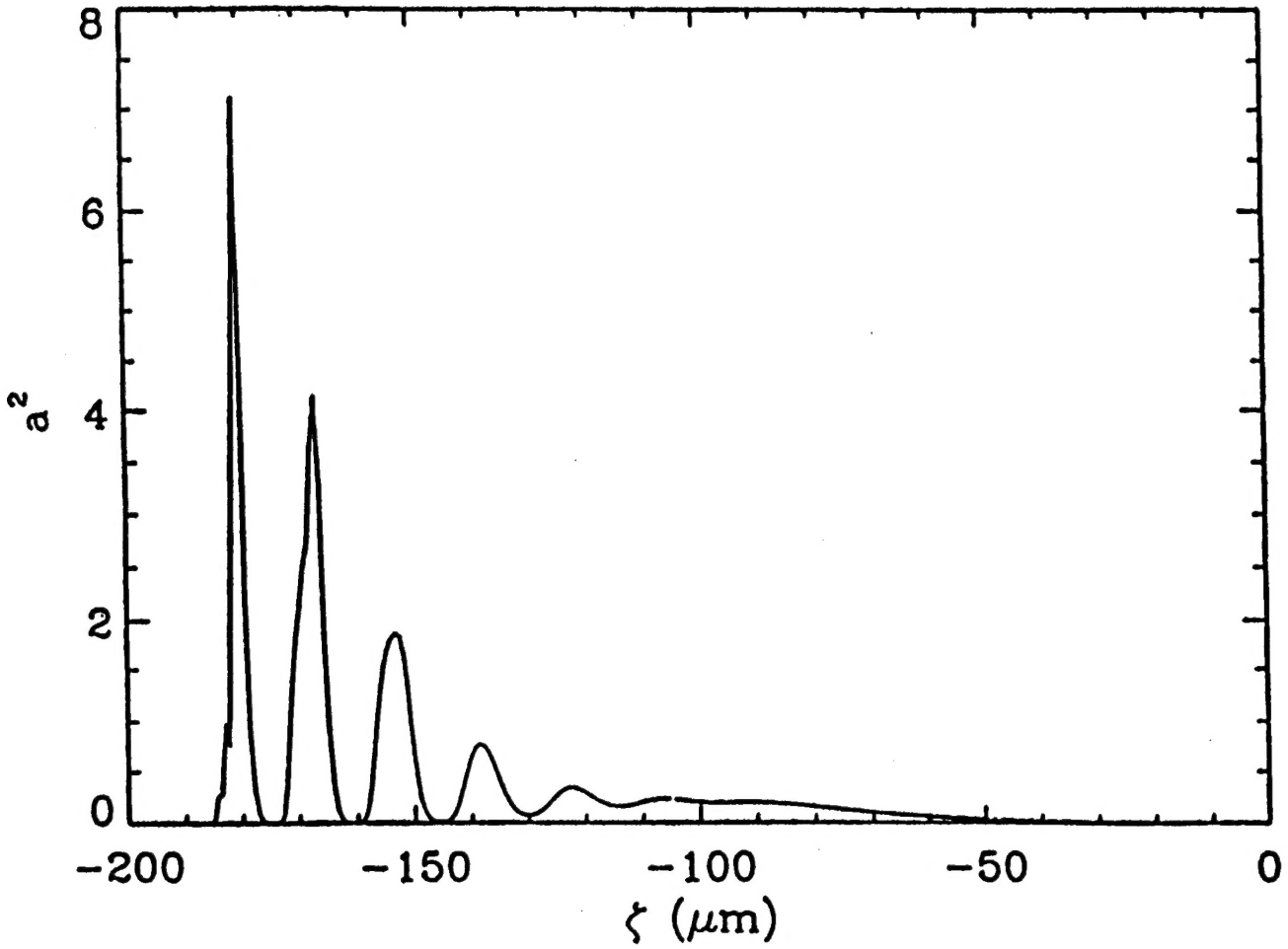

Fig. 5: Laser intensity $|\hat{a}_f|^2$ on-axis, versus ζ at $c\tau$ = 0.2 cm in the self-modulated LWFA. The NRL LWFA design parameters were used in this illustration.

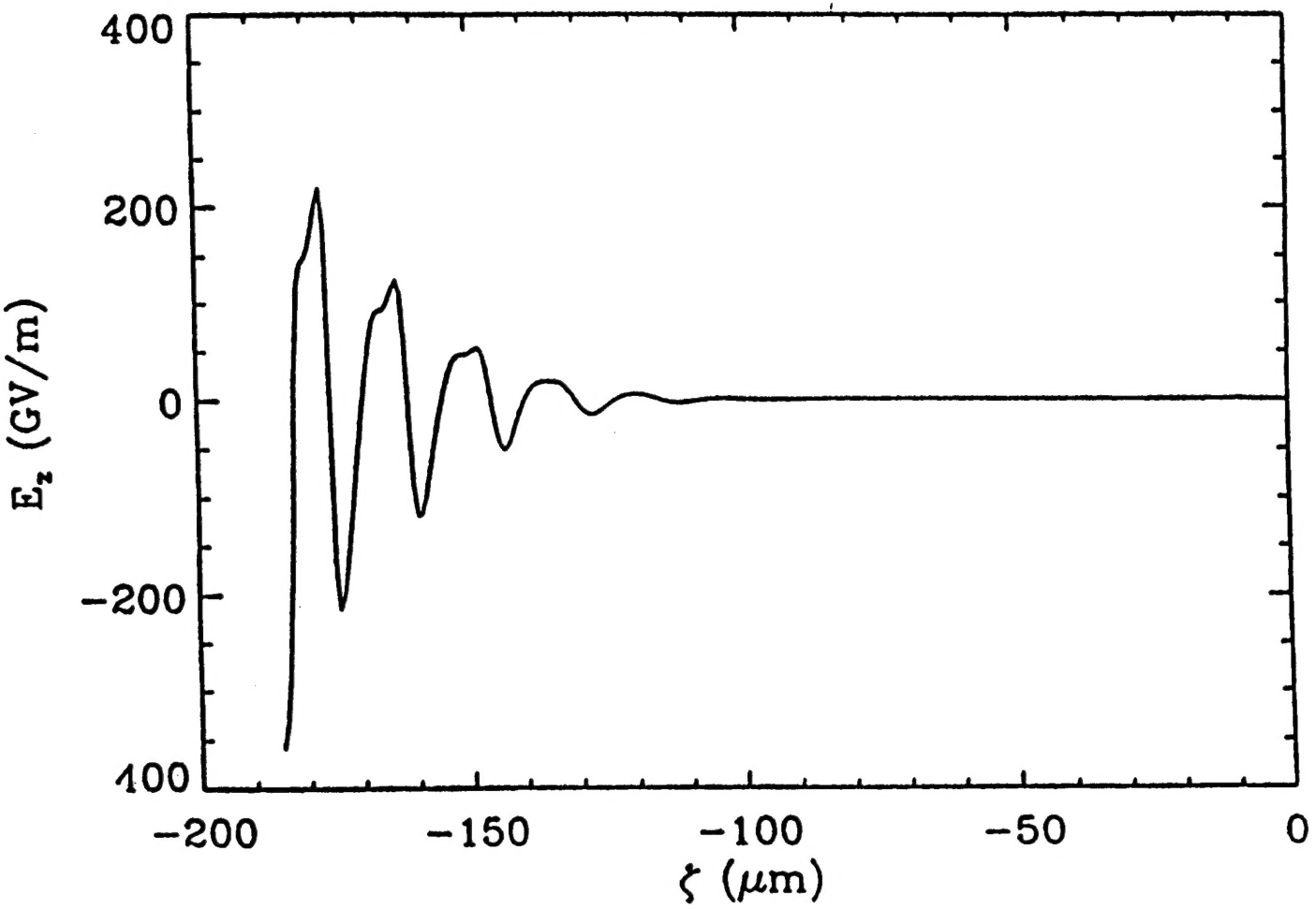

Fig. 6: Axial electric field E_z versus ζ at cτ = 0.2 cm.

FIGURE 6

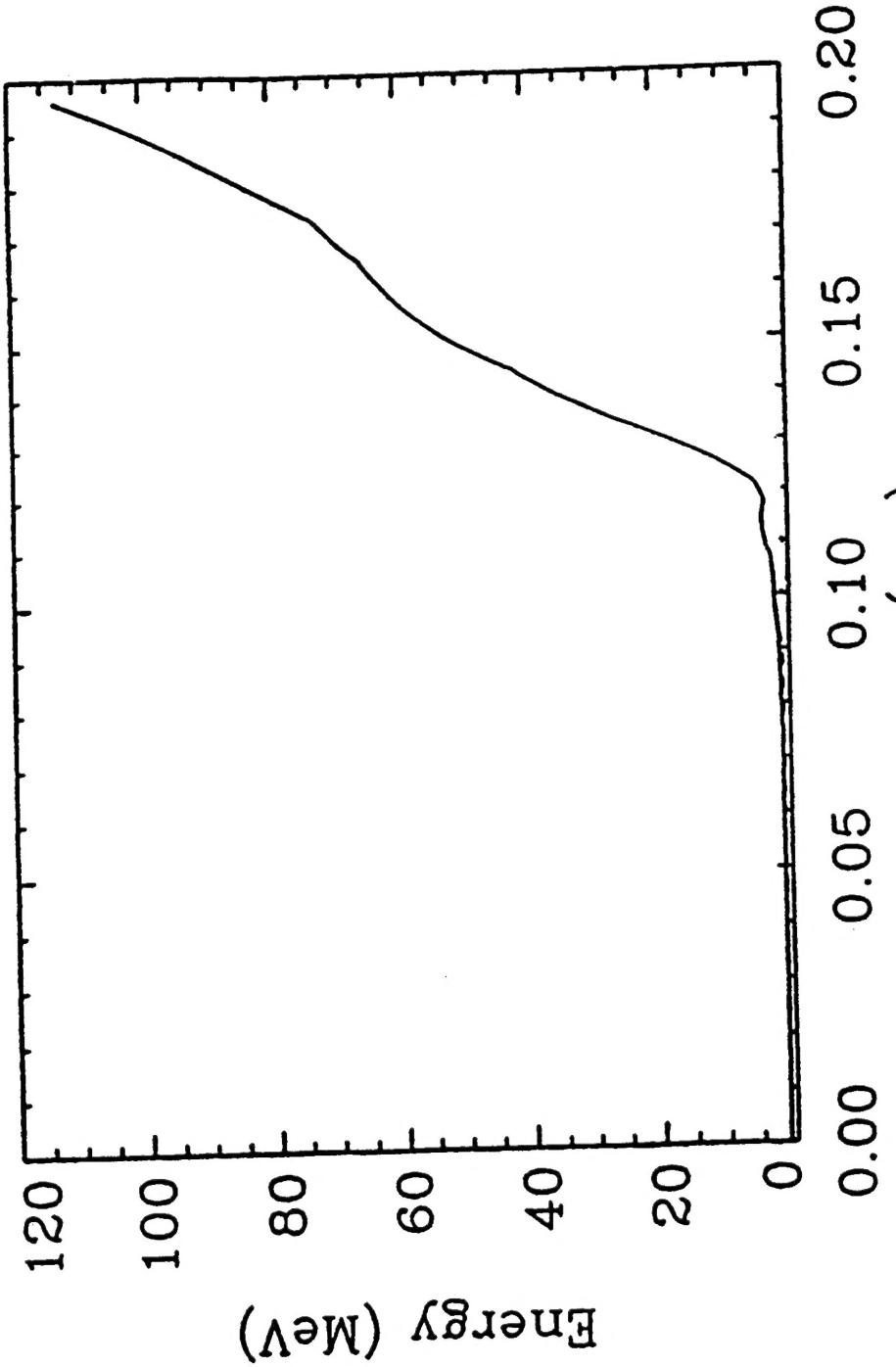

Fig. 7: Peak electron energy versus cτ for a beam with initial energy 1 MeV.